DAΦNE TECHNICAL NOTE
INFN - LNF, Accelerator Division

Frascati, June 6, 2006
Note: **I-17**

# FAST INJECTION KICKERS FOR DAΦNE AND ILC DAMPING RINGS

*D. Alesini, S. Guiducci, F. Marcellini, P. Raimondi*

## Abstract

In this paper we illustrate the design of new fast stripline kickers to inject or extract bunches in electron/positron rings. The kickers have been designed for the injection upgrade of the Phi-factory DAΦNE and as injection/extraction devices for the International Linear Collider (ILC) damping rings. The design is based on the idea to taper the striplines in order to simultaneously reduce the impedance of the device and to improve the deflecting field quality. The design has been done using 2D and 3D electromagnetic codes as Superfish and HFSS.

## 1. Introduction

The injection system is one of the challenging issues of the International Linear Collider (ILC) project [1] and the injection and extraction kickers are one of the most critical issues for the ILC Damping Rings [2]. In fact the bunch distance in the ring and therefore the choice of the ring circumference are related to the kicker pulse duration; moreover the stability of the beam position at the IP depends also on the kicker pulse stability. R&D programs are in progress in different laboratories at a global level both on the fast pulsers and on the stripline electrodes.

The injection and extraction kickers for the positron DR, which has a minimum bunch distance of 6.2 ns, should satisfy the following requirements:

a) Ultra short rise and fall time (total pulse duration < 12.4 ns);
b) High integrated strength;
c) Good uniformity of the deflecting field, within few percent over 90% of the beam stay clear;
d) Impedances of the structure as low as possible;
e) 3 MHz repetition rate.

There is a similarity between the ILC injected beam parameters and the DAΦNE ones, as shown in detail in sec. 2.1. Therefore stripline kickers studied for the ILC damping ring can be used for an upgrade of the DAΦNE injection system. The installation of these new kickers at DAΦNE is an important test for the ILC project, since it should demonstrate with beam measurements the achievement of the kicker performances. These kickers could also be used, in the framework of the ILC Collaboration, to test new fast pulsers produced by different laboratories or industry.

Compared to the present DAΦNE injection kickers the new ones have:

a) much shorter pulse ($\approx$12 ns instead of $\approx$150 ns);
b) better uniformity of the deflecting field;
c) lower impedance;
d) higher injection rate (max 50 Hz).

The much shorter pulse allows perturbing only the injected bunch and the two adjacent ones while, at present, a large fraction of the stored bunches (50/110 with 2.7 ns bunch spacing) are affected by the injection kick. This improvement, by reducing the perturbation of the kicker injection pulse on the stored bunches, can increase the current threshold of the transverse instability in the positron ring (as it has already been observed experimentally at DAΦNE). The better uniformity of the deflecting field can increase the injection efficiency at high currents and reduce the background to experiments during injection. The broadband impedance, according to the calculations, is reduced by a factor 3 with respect to the present kickers [3,4] (see sec. 3.3). Moreover, since the new kickers have been designed with the same beam pipe cross section of the dipoles, no tapers are needed between the dipoles and the kicker and this also contributes to the reduction of the machine impedance. Finally, the possibility of injection at 50 Hz can be useful for future upgrades of the whole injection system.

The design of the kickers is based on a tapered strip with rectangular cross section of the vacuum chamber in order to simultaneously achieve:

a) uniform transverse deflection as a function of the transverse coordinate;
b) tapered kicker structure (small device coupling impedance);
c) uniform beam pipe cross section between the dipole region and the kickers region.

In the paper we illustrate the design criteria and the obtained results.

## 2. General considerations on stripline kickers design

### *2.1 Pulse length requirements*

The total transverse deflecting voltage integrated by a particle, as a function of time, can be calculated from the kicker geometry and the input pulse shape. It is given by the convolution between the kicker impulse response[1] and the input pulse. In the ideal case, if the kicker has a constant transverse section, and matching between the pulse generator and the kicker structure is perfect, the kicker impulse response is a rectangular function of length 2L/c (see par. 2.2) where L is the kicker length, as shown in Fig. 1.

A simplified kicker input pulse profile is shown in Fig. 2a. The total deflecting field as a function of time related to this pulse is shown in Fig. 2b assuming of $T_f$>2L/c>$T_r$. With this model it is possible to do a first evaluation of the input pulse and kicker requirements in term of rise/decay time ($T_r$), flat-top time ($T_f$), and kicker length (L)([2]). The kickers parameters for the ILC positron damping rings and for DAΦNE are shown in Table 1. The pulse duration and kicker length have been chosen to obtain a flat top of the deflecting voltage equal to $4\sigma_B$ (assuming $T_r$=300 ps) and a total length of the deflecting voltage equal to $2T_B$ and $4T_B$ for ILC and DAΦNE respectively (see Fig. 3). The bunches near the deflected one, in the case of

---

[1] Given by the deflecting voltage, as a function of time, when the input pulse is a $\delta$ -function.

[2] The kicker length L is essentially determined by half the deflecting pulse duration (as seen by the bunches) multiplied by c, while the flat-top time $T_f$ by the pulse duration.

DAΦNE, receive a kick with an amplitude equal to half the amplitude of the kicked bunch, while, in the case of ILC, the two adjacent bunches are not kicked at all. It is straightforward to verify that there is similarity between the ILC kickers requirements and the DAΦNE ones. In particular, if we assume for the positron damping ring a horizontal $\beta$ -function at the kicker equal to 70 m, the total required deflecting voltage, the kicker length and the pulse length are almost the same in the two cases. Also the horizontal beam stay clear at the kicker is the same.

Table 1: Kicker and input pulse parameters for ILC Damping Rings and DAΦNE

| | ILC DR(*) | DAΦNE |
|---|---|---|
| Energy E [GeV] | 5 | 0.51 |
| Time spacing between bunches $T_B$ [ns] | 6.2 | 2.7 |
| Bunch length $\sigma_B$ [mm] | 6 | 35 |
| Deflection [mrad] | 0.7 | 5 |
| Total deflecting voltage $V_T$ [MV] | 3.5 | 2.5 |
| kicker length L [cm] | 87 | 73 |
| Flat top pulse length $T_f$ [ns] | 5.9 | 5.3 |
| Horizonthal beam stay clear @ kicker (diameter) [mm] | 50 | 50 |

*referred to the positron ring with horizontal $\beta$ -function at the kicker equal to 70 m.

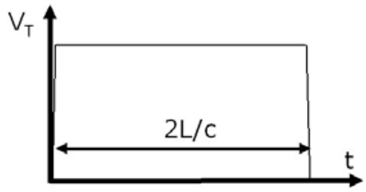


Figure 1: Ideal kicker impulse pulse response.

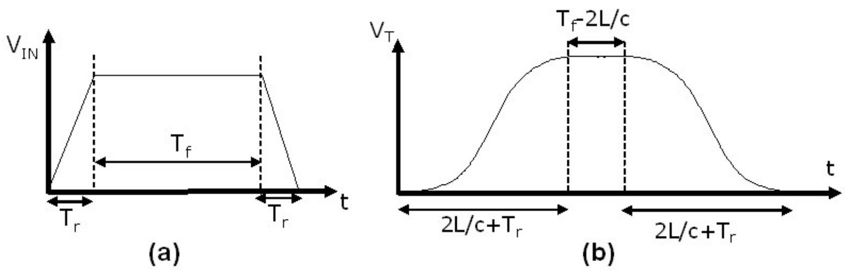


Figure 2: (a) Simplified kicker input pulse profile; (b) Total deflecting field as a function of time assuming of $T_f$>2L/c>$T_r$.

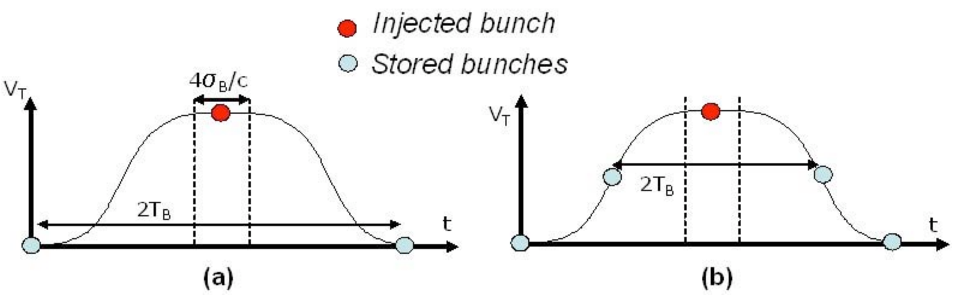


Figure 3: Total deflecting field as a function of time in the ILC (a) and in the DAΦNE (b) case.

### *2.2 Transverse field profile properties*

A cross section of a general stripline (one quarter of the structure) is sketched in Fig. 4 with the electric and magnetic field lines of the TEM deflecting mode[3]. The mode can be excited by feeding the two strips with opposite voltages while the particle beam travels in the opposite direction with respect to the TEM wave[4]. For a given stripline aperture (*a*) it is possible to calculate the total equivalent deflecting field $E_T$ at the center of the structure, normalized to the input voltage $V_{strip}$([5]), as a function of the half-coverage angle $\phi$. The result obtained with Superfish [5] is plotted in Fig. 5 assuming a = 25mm and the impedance of each strip equal to $50\Omega$. As expected, the intensity of the deflecting field increases if we increase the angle $\phi$. In fact the deflection in the center of the pipe is given, to first order, by the combination of two opposite contributions: the strip currents and their images on the vacuum chamber. If we increase the coverage angle we reduce the contribution of the currents on the surface of the vacuum chamber because, in order to maintain the strip impedance constant, we have to increase the distance between the strip and the vacuum chamber itself (for example $\phi = 70°$ needs *h* =50 mm).

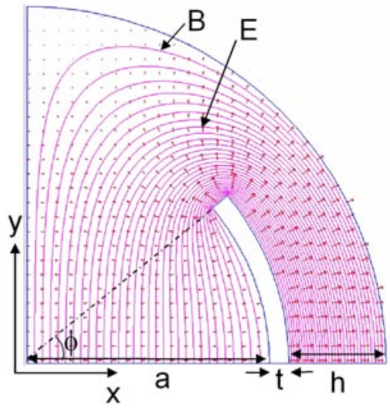


Figure 4: Cross section of a circular stripline (one quarter of the structure) with the electric and magnetic field lines of the TEM deflecting mode.

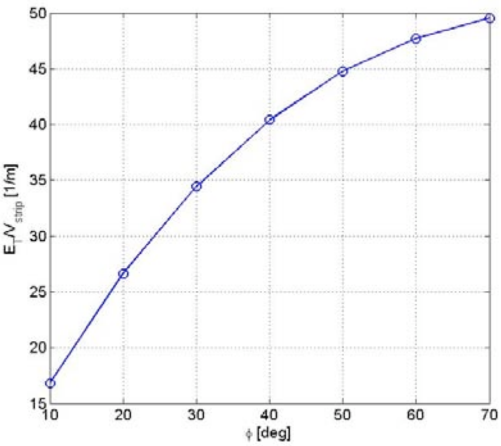


Figure 5: Total equivalent deflecting field $E_T$ at the center of the structure, normalized to the input voltage $V_{strip}$, as a function of the half-coverage angle $\phi$.

[3] x is the horizontal coordinate, y is the vertical and z is the longitudinal.

[4] In this way the contributions of the electric and magnetic deflections add each other. In the case of a beam traveling at the velocity of light, in fact, the two contributions have exactly the same amplitude. In the case of a beam traveling in the same direction as the TEM wave, the electric and magnetic deflections cancel each other.

[5] We define $V_{strip}$ as the voltage given to each strip.

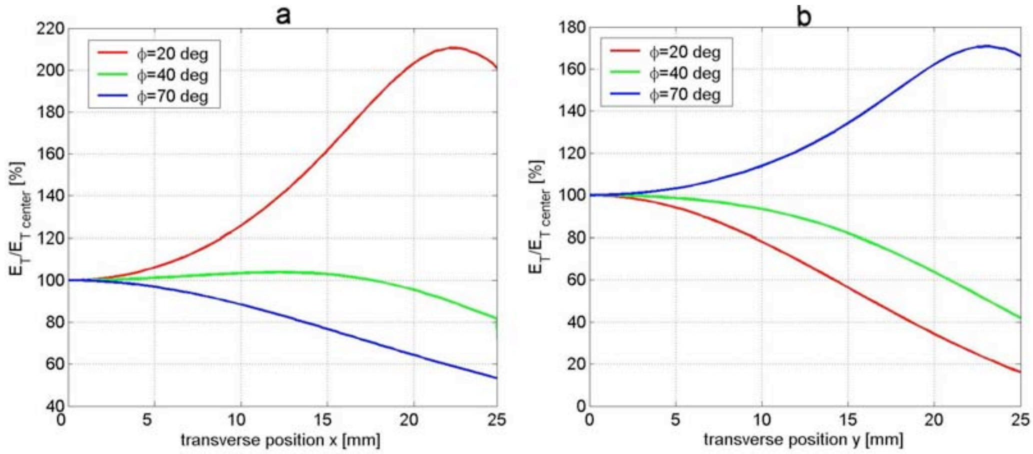


Figure 6: Deflecting field normalized to its value at the center of the pipe, as a function of the transverse coordinates.

Another important point to be taken into account is the behaviour of the deflecting field as a function of the transverse coordinates (*x,y*). The plot of the deflecting field normalized to its value at the center of the pipe, as a function of the horizontal coordinate is given in Fig. 6a for three different values of the coverage angle. There is a different behaviour in the three cases: for small values of $\phi$, the deflecting field increases with $x$ while, for large values of $\phi$, it decreases. This comes from by the fact that, for small values of the coverage angle the field generated by the strip is similar to that of a simple wire, while, for large values there is a shielding effect of the deflecting field given by the strip itself. The optimum case is represented by $\phi \cong 40\,\mathrm{deg}$ even if, also in this case, the variation of the deflecting field as a function of the horizontal coordinate can be few tens of percent inside the good field region. In Fig. 6b we have plotted the same quantity as a function of the vertical coordinate $y$. In this case the behaviour is opposite: for small values of $\phi$ the intensity decreases because we go far from the strip, while, for large values of $\phi$, the edge effects of the strip give a local increase of the field.

An elliptical strip section and the related electromagnetic field lines are reported in Fig. 7. The normalized deflecting field as a function of the coverage angle is given in Fig. 8 and compared to the case of a circular strip. For large coverage angles, the efficiency of an elliptical stripline is larger than the circular one because of the proximity of the strip current to the center of the pipe. On the other hand for large values of the coverage angle, the deflecting field strongly decreases if we move from the center of the pipe toward the strip following the $x$ direction and it strongly increases if we move from the center toward the $y$ direction (see Fig. 9).

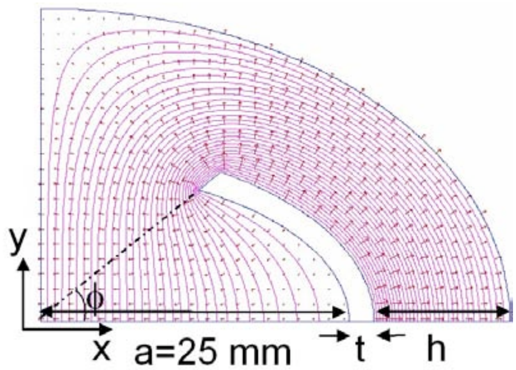


Figure 7: Example of transverse section of an elliptical strip and electromagnetic field lines.

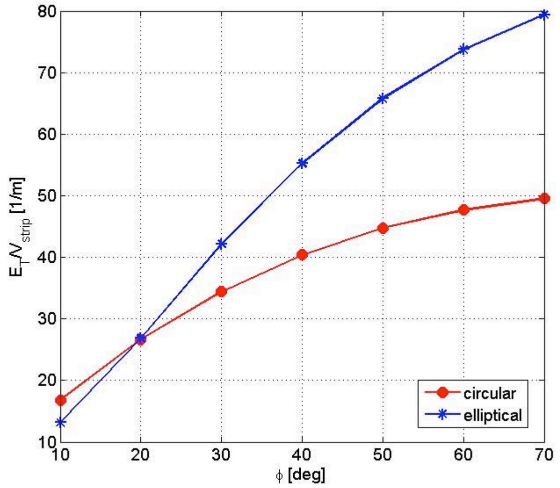


Figure 8: Normalized deflecting field as a function of the coverage angle for an elliptical stripline.

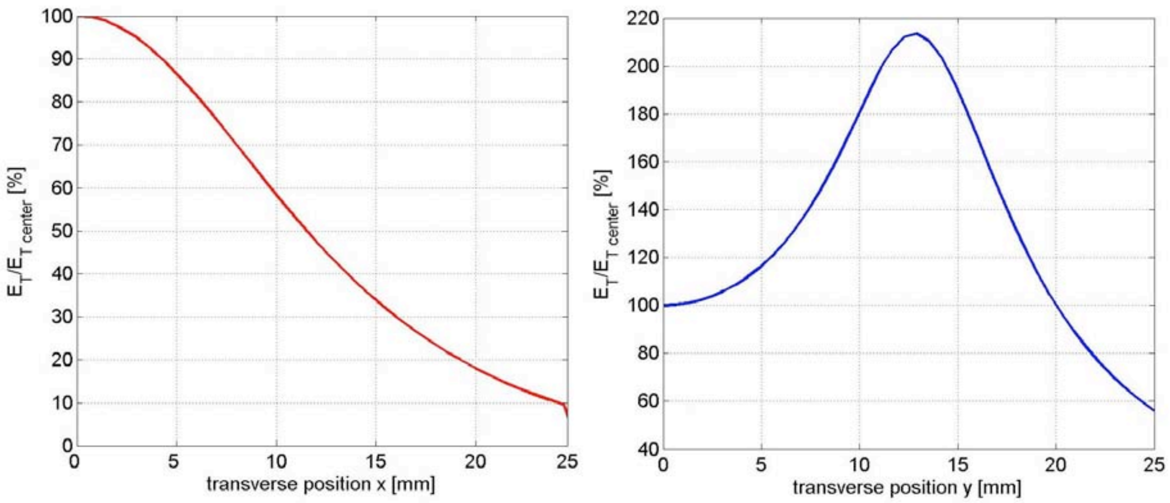


Figure 9: Deflecting field normalized to its value on the center of the pipe, as a function of the transverse coordinates (elliptical case with $\phi = 70\,\text{deg}$).

## 3. Design of the stripline injection kickers

The design of the new kickers is based on the idea to properly taper the striplines of the kickers. Two sketches of possible tapered geometries are shown in Fig. 10. Each transverse section should have constant impedance in order to avoid reflections of the input pulse.
The tapered striplines allow to:

a) reduce the broadband beam coupling impedance of the device;
b) improve the deflecting field quality obtaining a uniform transverse deflection as a function of the transverse coordinate (horizontal in particular);
c) obtain a better matching between the generator and the kicker structure at high frequency[6];
d) reduce the beam transfer impedance.

[6] This can avoid multiple reflections of the deflecting pulse in the kicker structure that can perturb the stored bunches especially in the ILC case.

The tapered scheme is applicable to both circular and elliptical geometries.

Concerning the uniformity of the deflecting field as a function of the transverse coordinate, it should be pointed out that the behaviour of the deflecting field depends on the coverage angles (see par. 2.1). The length of the tapers with respect to the central region can be therefore optimized in order to obtain a uniform integrated deflecting field along the horizontal coordinate *x*. The sections with small coverage angle, in fact, compensate the reduction of the deflecting field near the strip, given by the large coverage angle of the central part of the kicker.

The small discontinuity at the entrance and exit of the kicker given by the proximity of the strip to the vacuum chamber assures a better matching between the pulse generator and the kicker structure, especially at high frequency, and reduces the longitudinal and transfer impedance of the device [6].

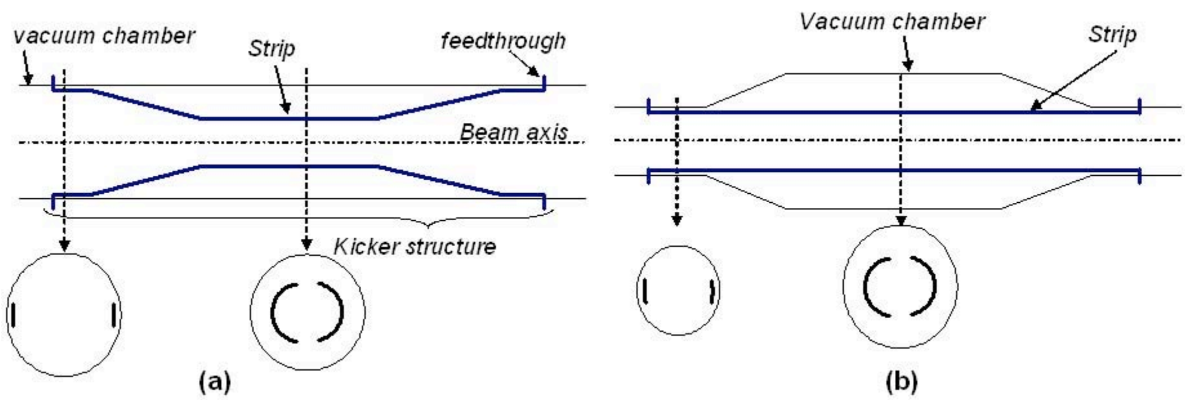


Figure 10: Sketches of different tapered stripline kickers.

### *3.1 DAΦNE injection kicker design*

As shown in sec. 2.1 the kicker requirements for the ILC DR and for DAΦNE are similar. In the following we will refer in particular to the case of DAΦNE even if the same results can be applied to the ILC case with minor modifications.

To reduce the broadband impedance of the whole accelerator, an elliptical-like geometry has been chosen to have a minimum variation of the vertical dimension of the beam pipe between the dipole and the injection regions (see Fig. 11). The general cross section of the kicker is sketched in Fig. 12 and the final optimized kicker dimensions are shown in Fig. 13:

a) each section of the kicker has the same Dh in order to not have a transverse modulation of the horizontal kicker vacuum chamber;
b) the value of a, b and t are the same for each section;
c) the D and Dv dimensions[7] have a linear modulation along the kicker;
d) the value of $\phi$ is progressively increased along the kicker up to 90 deg. (in the central part of the kicker) maintaining a constant 50 Ω impedance in each section (equal to the output impedance of the pulsers);
e) the value of a and b have been optimized together with the length of the central part of kicker and tapers in order to achieve at the same time an optimum deflecting field uniformity as a function of the horizontal coordinate and a total electrical length of the kicker compatible with the bunch spacing as illustrated in par. 2.1.

---

[7] Representing the distance of the strip from the beam axis (since a is constant) and the half height of the kicker vacuum chamber, respectively.

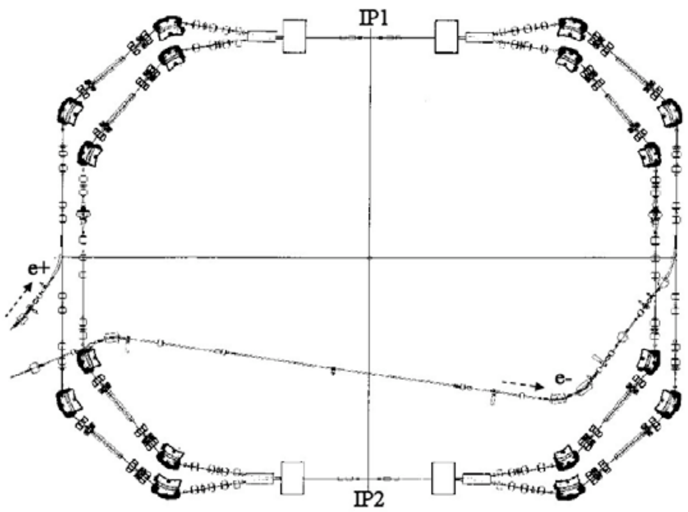


Figure 11: Sketch of the DAΦNE main rings.

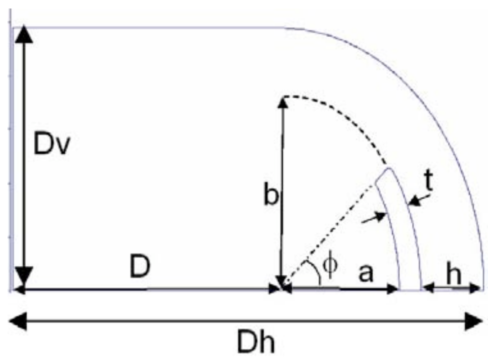


Figure 12: Generic cross section of the kicker.

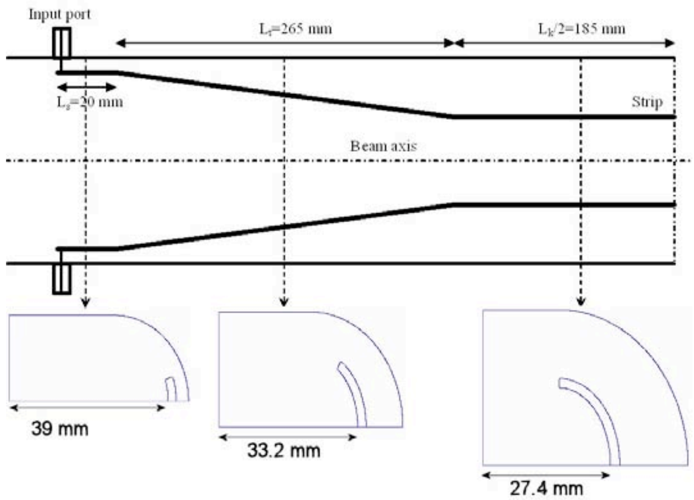


Figure 13: Final optimized dimensions of the kicker (half structure).

The deflecting field as a function of the longitudinal and horizontal coordinates is shown in Fig. 14. The map has been obtained by simulating 2D profiles with Poisson-Superfish at different cross sections of the kicker and constructing the 3D map of the total deflecting field by interpolating the profiles at the different sections. This procedure allowed to strongly reduce the computational time needed to optimize the geometry of the structure. In particular, with this method the ratio between the length of the tapered structure and of the central part of the kicker has been optimized in order to achieve an optimum deflecting field uniformity in the horizontal coordinate. The deflecting field, as a function of the transverse coordinates, is given in Fig. 15.

Since the tapers reduce the efficiency of the structure and, therefore, increase the required voltage per strip, it has been preferred to increase the total length of the device even if it implies a longer total pulse length. With a signal of the type sketched in Fig. 16a, which reproduces schematically the input signal from the pulser, the total deflecting field as a function of time is shown in Fig. 16b and the required voltage is about 45 kV. In this case also the two bunches that are 5.4 ns away from the injected one, receive a small kick.

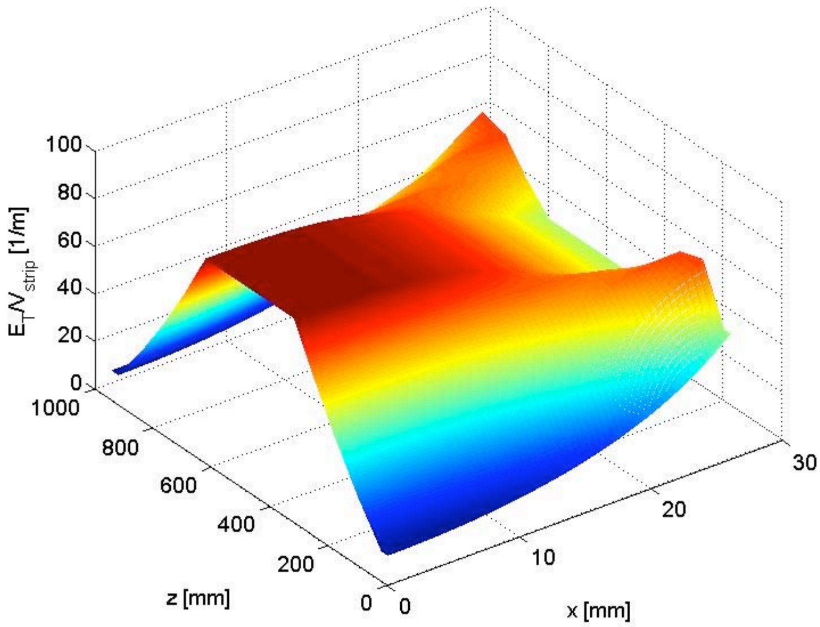


Figure 14: 2D map of the deflecting field as a function of the longitudinal and horizontal coordinates obtained by Superfish.

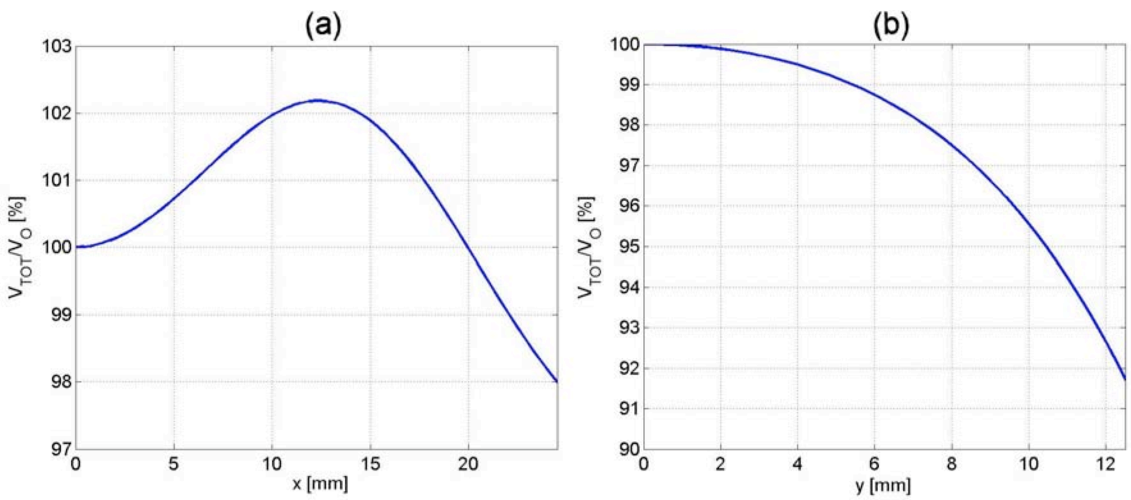


Figure 15: Deflecting field as a function of the transverse coordinates.

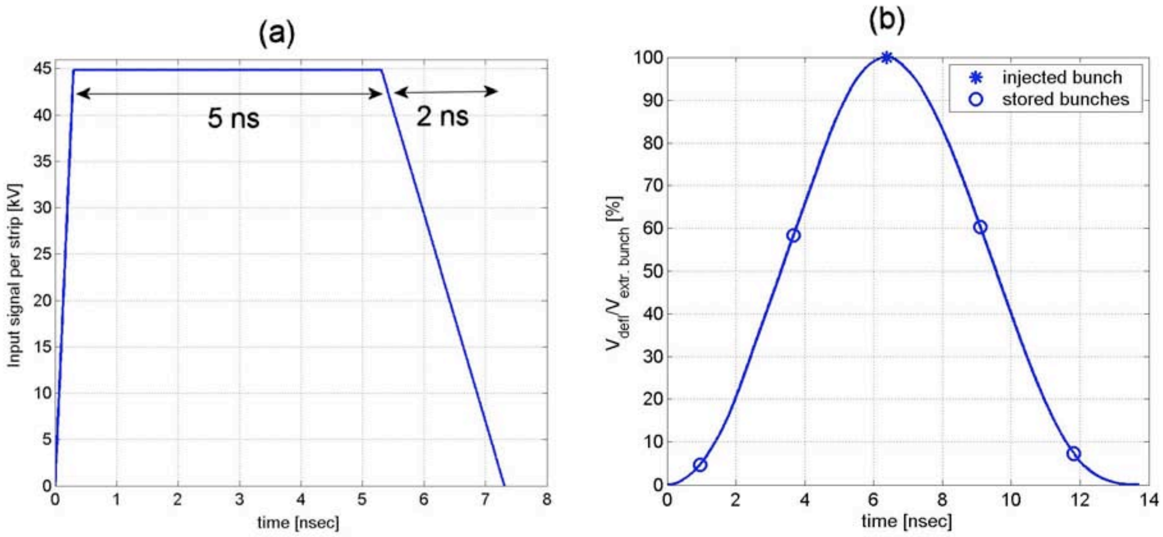


Figure 16: (a) Input pulse signal profile and related total deflecting field as a function of time (b).

### *3.2 3D simulations and final optimization*

The HFSS [7] 3D model of the kicker is shown in Fig. 17. With the 3D code it is possible to optimize the design to:

a) evaluate the effects due to the presence of the ceramic stand-offs supporting the strips;

b) optimize the transition between the coaxial feedthrough and the kicker structure.

The calculated reflection coefficient at the input port with and without the ceramic stand-off is given in Fig. 18a. The slightly worst response at high frequencies is related to the frequency content of the input signal of Fig 18b: the calculations give a tolerable reflected power of the order of a fraction of percent.

With the 3D code we have also calculated the deflecting field as a function of the transverse coordinates. The results are shown in Fig. 19 and compared with the 2D calculations.

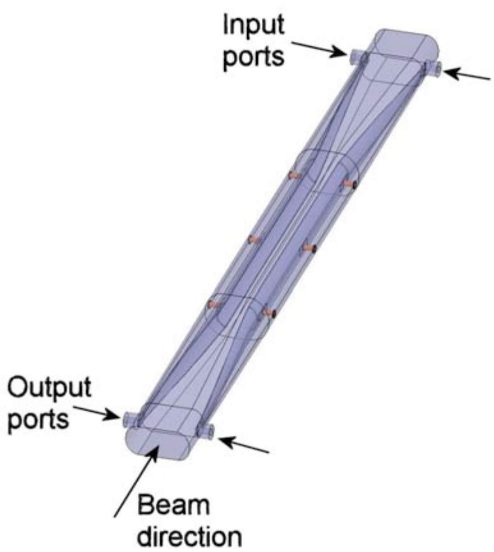


Figure 17: HFSS 3D model of the kicker.

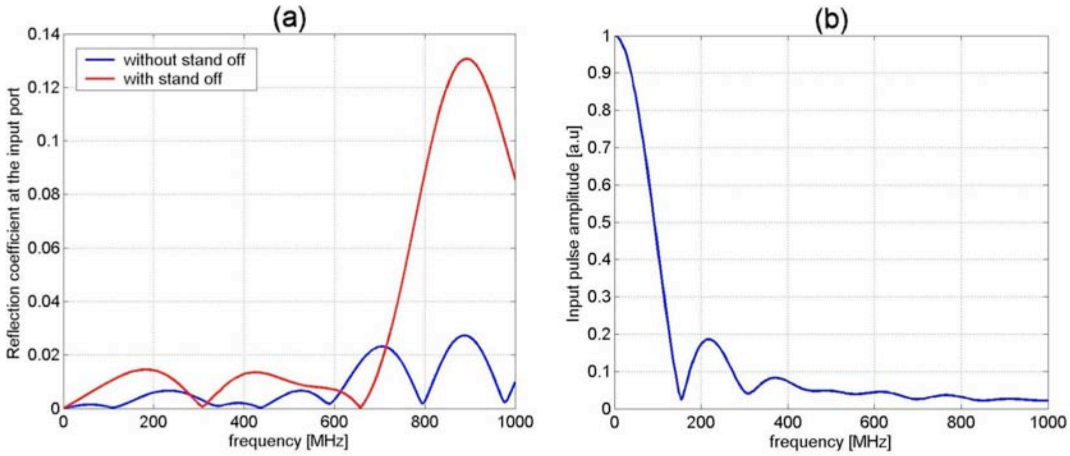


Figure 18: (a) Calculated reflection coefficient at the input port with and without the ceramic stand off; (b) Normalized Fourier transform of the input signal.

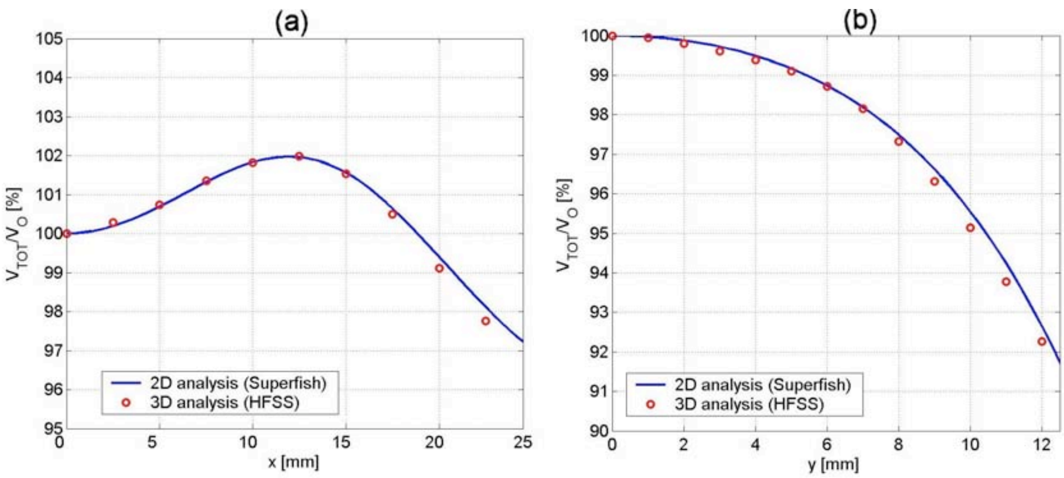


Figure 19: Uniformity of the deflecting field as a function of the transverse coordinates (HFSS results).

### *3.3 Kicker beam coupling impedance and beam transfer impedance evaluation*

With HFSS we have also calculated:

a) the longitudinal and transverse beam coupling impedances of the structure;

b) the beam transfer impedance.

The longitudinal and transverse beam coupling impedances have been calculated with the wire method [8] using HFSS. The simulated structure is reported in Fig. 20. Since the port connected to the input pulser can not be considered as perfectly matched, the longitudinal and horizontal impedances have been calculated in two different cases: a perfect matched pulser port and an open pulser one[8]. The results of the impedance calculation are plotted in Figs. 21 and 22. No higher order modes (HOM) are trapped in the structure. The loss factors $k_l$ are given in Table 2 for different bunch length.

Concerning the vertical impedance, four vertical modes are trapped in the structure as shown in Fig. 23. Their field configuration and parameters are given in Fig. 24 and in Table 3.

[8] The "real" load will be something in between the two cases.

Since the modes are $TE_{11n}$ like modes, their transverse impedances are very low and the resulting growth rates (in the DAΦNE case), supposing a full coupling with a coupled bunches mode, are of the order of 1 $ms^{-1}$ at a total current of 2A, about two order of magnitude lower than the damping rates provided by the DAΦNE vertical feedback system.
The beam transfer impedance between the beam and the downstream (pulser) and upstream (load) ports are shown in Fig. 25. From the results it is possible to evaluate the peak voltage into the ports and the average power for a given beam current. The results are given in Table 4 and 5 for different beam currents.

Table 2: Loss factor due to the kicker for different bunch length.

| Bunch length [cm] | $k_l$ [V/pC] |
|---|---|
| 1 | $5\cdot 10^{-3}$ |
| 2 | $4.8\cdot 10^{-3}$ |
| 3 | $4.6\cdot 10^{-3}$ |

Table 3: Parameters of the vertical modes trapped in the kicker.

| MODE | Frequency [GHz] | Q | RT [$k\Omega/m$] |
|---|---|---|---|
| $TE_{111}$ | 1.5992 | 6987 | 28.2 |
| $TE_{112}$ | 1.657 | 6960 | 2.9 |
| $TE_{113}$ | 1.7379 | 6836 | 45.7 |
| $TE_{114}$ | 1.8227 | 6914 | 12.6 |

Table 4: Peak voltage into the upstream and downstream ports induced by the beam.

| Bunch Charge [nC] | Peak voltage into the downstream port [V] | Peak voltag into the upsteram port [V] |
|---|---|---|
| 1 | 8 | 16 |
| 3 | 25 | 50 |
| 6 | 50 | 100 |

Table 5: Average power into the upstream and downstream ports induced by the beam.

| Beam current [A] | Average power into the downstream port [W] | Average power into the upsteram port [W] |
|---|---|---|
| 1 | 1 | 5 |
| 2 | 4 | 20 |

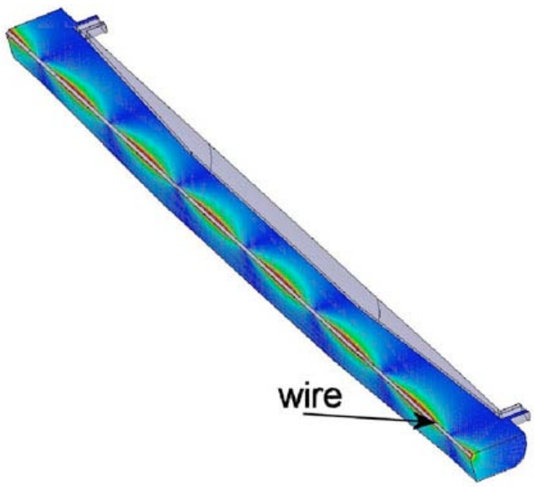


Figure 20: HFSS simulated structure with a central wire.

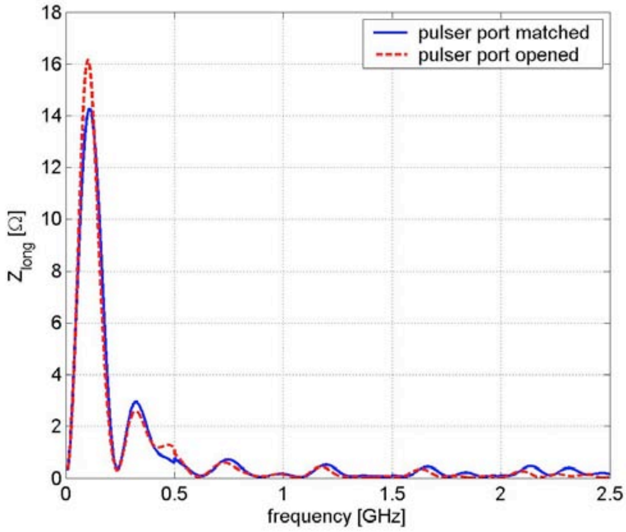


Figure 21: Longitudinal impedance calculated by HFSS (wire method).

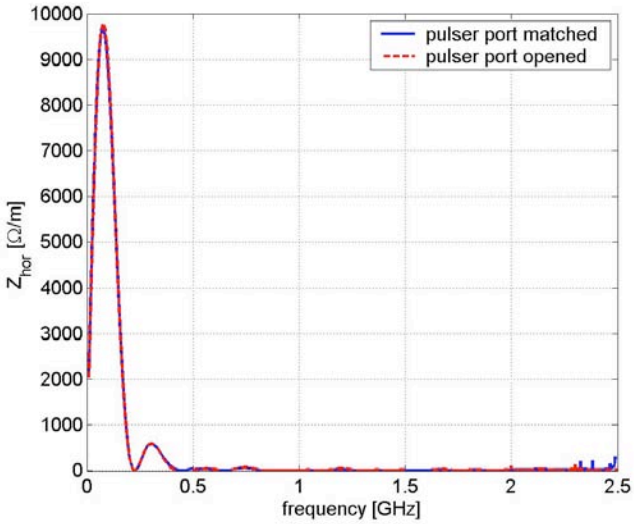


Figure 22: Horizontal impedance calculated by HFSS (wire method).

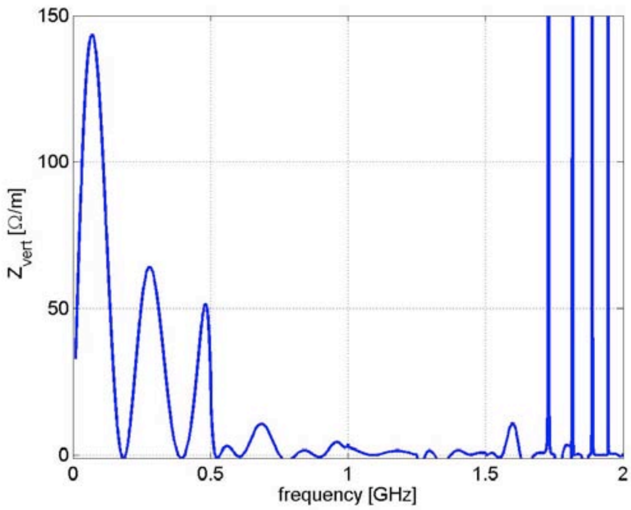


Figure 23: Vertical impedance calculated by HFSS (wire method).

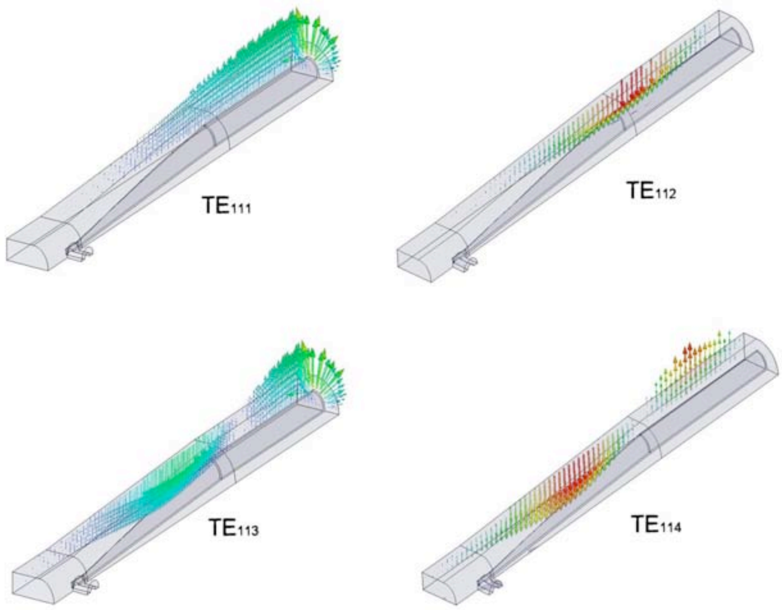


Figure 24:Transverse vertical mode trapped in the kicker.

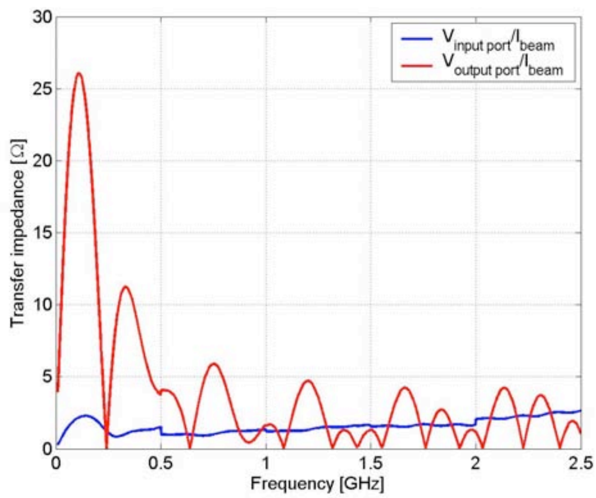


Figure 25: Transfer impedance calculated by HFSS.

### *3.4. ILC kickers*

The kicker design can be applied, with minor modifications, to the ILC positron damping ring. Assuming a 3 MHz and 5 kV input pulse per strip, the total required number of kicker is $\approx 12$.

## 4 Conclusions

We have illustrated the design of new fast stripline kickers to inject or extract bunches in electron/positron rings. The kickers have been designed for the injection upgrade of the Phi-factory DA$\Phi$NE and as injection/extraction devices for the International Linear Collider (ILC) damping rings. The design is based on the concept of tapering the striplines in order to simultaneously reduce the impedance of the device and to improve the deflecting field quality. The design has been done using 2D and 3D electromagnetic codes such as Superfish and HFSS.

The required voltage per strip is about 45 kV and the uniformity of the deflecting field as a function of the horizontal coordinate is of the order of ± 2% over all the kicker horizontal aperture while it is less than 10 % over ± 1 cm along the vertical coordinate.
No longitudinal and horizontal HOMs are trapped in the structure and the longitudinal loss factor is about $5 \cdot 10^{-3}$ V/pC for 1 cm bunch length. Concerning the vertical impedance four HOM are trapped in the structure with a vertical impedance of the order of few tens of kV per meter.

The maximum induced peak voltage on the upstream port is of the order of 100 V with a 6 nC bunch while the average power induced on the ports is of the order of few tens of Watts with a 2 A beam.

## Acknowledgements

We would like to thank M.A. Preger, C. Sanelli, A. Gallo and M. Zobov for helpful discussions and suggestions.

This work is supported by the Commission of the European Communities under the 6th Framework Programme "Structuring the European Research Area", contract number RIDS-011899.

## References

[1] S. Guiducci, "Progress and plans for R&D and the Conceptual Design of the ILC Injector Systems", PAC05, Knoxville, (USA), May 2005;

[2] A. Woslki, J. Gao, S. Guiducci editors, "Configuration Studies and Recommendations for the ILC Damping Rings", LBNL–59449, Cockroft–06–04, February 2006, available at http://www.desy.de/~awolski/ILCDR/DRConfigurationStudy_files/DRConfigRecommend.pdf

[3] S. De Simone and A. Ghigo, "DAΦNE Accumulator Kickers", EPAC 92, Berlin, March 1992.

[4] M. Zobov et al., "Collective Effects and Impedance Study for the DAΦNE Φ-Factory", LNF-95-041(P), 1995.

[5] Poisson Superfish, James H. Billen and Lloyd M. Young, software produced under U.S. Government by Los Alamos National Laboratory, Particle Accelerators 7 (4), 213-222 (1976).

[6] D.A. Goldberg and G.R. Lambertson, "Dynamic Devices: A Primer On Pickups and Kickers", LBL-31664 ESG-160, 1992.

[7] www.ansoft.com.

[8] F. Caspers, "Impedance determination: bench measurements", in Handbook of Accelerator Physics and Engineering edited by A.W. Chao and M. Tigner, World Scientific, 1999.